Controlling neuronal spikes

Sudeshna Sinha
The Institute of Mathematical Sciences, CIT Campus, Madras 600 113, India

William L. Ditto
Georgia Tech/Emory Biomedical Engineering Department, 315 Ferst Drive, Atlanta, Georgia 30332-0535

(Received 24 August 2000; published 18 April 2001)

We propose two control strategies for achieving desired firing patterns in a physiologically realistic model neuron. The techniques are powerful, efficient, and robust, and we have applied them successfully to obtain a range of targeted spiking behaviors. The methods complement each other: one involves the manipulation of only a parameter, the applied soma current, and the other involves the manipulation of only a state variable, the membrane potential. Both techniques have the advantage that they are not measurement-intensive nor do they involve much run-time computation, as knowledge of only the interspike interval is necessary to implement control.

DOI: 10.1103/PhysRevE.63.056209 PACS number(s): 05.45.Gg, 84.35.+i, 07.05.Mh, 87.19.La

I. INTRODUCTION

A wide range of phenomena occurs in nature and in the laboratory, ranging from highly coherent ones such as synchronized oscillator arrays to highly disordered systems such as seen in fluid turbulence. Control mechanisms that enable a system to maintain a fixed activity (the ''goal'' or ''target'') even when intrinsically chaotic have many applications in situations ranging from biology (as in the control of cardiac rhythms) to engineering [1]. In neuronal systems, in particular, a wealth of complex patterns has been experimentally observed in a variety of cases [2]. However, the mechanisms by which such complex spiking patterns can be manipulated are not well understood. It is thus of considerable interest and potential utility to *device control algorithms capable of achieving the desired type of behavior* in such complex systems. In this paper, we offer two complementary control strategies targeting desired firing patterns in a prototypical model of a Hippocampal neuron: the Pinsky-Rinzel model [3]. First we describe the model neuron below.

II. THE PINSKY-RINZEL MODEL NEURON

Based on extensive physiological data, Traub developed a 120-variable 19-compartment model of a pyramidal cell from the CA3 region of the hippocampus of the brain [4]. Subsequently, Pinsky and Rinzel reduced this to an eight-variable two-compartment model while still preserving its physiological relevance [3]. This is the model that we will use to explore ways of manipulating the responses of the neuron.

The Pinsky-Rinzel model neuron consists of somatic and dendritic compartments resistively coupled at different potentials. A patch of the cell membrane is modeled as an equivalent electrical circuit consisting of a resistor and a capacitor in parallel. The current balance equations for the two compartments follow from differentiating the capacitance definition. The details of the model, the values of the parameters, and initial conditions are given below [5].

The eight variables in the model are the five gating variables h, n, s, c, and q; the Ca level [Ca]; and the soma voltage V_s and dendrite voltage V_d. The parameters include the coupling conductance between soma and dendrite g_c, reversal potentials V_{Na}, V_{Ca}, V_{K}, V_l, V_{syn}, ionic conductances g_l, g_{Na}, g_{KDR}, g_{Ca}, g_{KAHP}, g_{KCa}, synaptic conductances g_{MMDA}, g_{AMPA}, relative area of soma to dendrite p, membrane capacitance c_m, and the applied soma current i_s.

The gate equations are of the form

$$\frac{dh}{dt}=(1-h)\alpha_h-h\beta_h, \tag{1}$$

$$\frac{dn}{dt}=(1-n)\alpha_n-n\beta_n, \tag{2}$$

$$\frac{ds}{dt}=(1-s)\alpha_s-s\beta_s, \tag{3}$$

$$\frac{dc}{dt}=(1-c)\alpha_c-c\beta_c, \tag{4}$$

$$\frac{dq}{dt}=(1-q)\alpha_q-q\beta_q, \tag{5}$$

where α and β are phenomenologically determined from experimental data so as to mimic the opening and closing of membrane gates [3]:

$$\alpha_h=0.128\exp\left(\frac{17.0-V_s}{18.0}\right), \tag{6}$$

$$\beta_h=4.0\Big/\left\{1.0+\exp\left(\frac{40.0-V_s}{5.0}\right)\right\}, \tag{7}$$

$$\alpha_n=0.016(35.1-V_s)\Big/\left[\exp\left(\frac{35.1-V_s}{5.0}\right)-1.0\right], \tag{8}$$

$$\beta_n = 0.25 \exp(0.5 - 0.025 V_s), \tag{9}$$

$$\alpha_s = \frac{1.6}{1.0 + \exp[-0.072(V_d - 65.0)]}, \tag{10}$$

$$\beta_s = 0.02(V_d - 51.1) \Big/ \left\{ \frac{\exp(V_d - 51.1)}{5.0} - 1.0 \right\}, \tag{11}$$

$$\alpha_c = \left\{ \exp\left(\frac{V_d - 10.0}{11.0} - \frac{V_d - 6.5}{27.0} \right) \right\} \Big/ \ 18.975 \quad \text{if } V_d \leqslant 50.0, \tag{12}$$

$$\beta_c = 2.0 \exp\left(\frac{6.5 - V_d}{27.0} \right) - \alpha_c \quad \text{if } V_d \leqslant 50.0, \tag{13}$$

$$\alpha_c = 2.0 \exp\left(\frac{6.5 - V_d}{27.0} \right) \quad \text{if } V_d > 50.0, \tag{14}$$

$$\beta_c = 0.0 \quad \text{if } V_d > 50.0, \tag{15}$$

$$\alpha_q = \min(0.000\,02[\mathrm{Ca}], 0.01), \tag{16}$$

$$\beta_q = 0.001, \tag{17}$$

$$\alpha_s = \frac{0.32(13.1 - V_s)}{\exp\left\{ \frac{(13.1 - V_s)}{4.0} - 1.0 \right\}}, \tag{18}$$

$$\beta_s = \frac{0.28(V_s - 40.1)}{\exp\left\{ \frac{(V_s - 40.1)}{5.0} - 1.0 \right\}}, \tag{19}$$

$$\tau_m = \frac{1}{\alpha_m + \beta_m}, \tag{20}$$

$$m_\infty = \alpha_m \tau_m . \tag{21}$$

The Ca level is given by

$$\frac{d[\mathrm{Ca}]}{dt} = -0.075[\mathrm{Ca}] - 0.13 s^2 g_{\mathrm{Ca}}(V_d - V_{\mathrm{Ca}}), \tag{22}$$

The rate of change of the soma and dendrite voltage is given by differentiating the capacitance definition $CV = Q = \Sigma I$, where a typical current is obtained from $IR = r(V - V_{\mathrm{ref}})$, where r is the voltage-dependent gating variable:

$$\frac{dV_s}{dt} = \frac{i_s}{c_m}, \tag{23}$$

$$\frac{dV_d}{dt} = \frac{i_d}{c_m}, \tag{24}$$

where i_s is a sum of the electronic coupling $-g_c(V_s - V_d)/p$, leak current $-g_l(V_s - V_l)$, inward Na current $-g_{\mathrm{Na}} m_\infty^2 h(V_s - V_{\mathrm{Na}})$, delayed-rectifier K current $-g_{\mathrm{KDR}} n(V_s - V_{\mathrm{K}})$, and soma electrode current i_s/p:

$$i_s = -g_c \frac{(V_s - V_d)}{p} - g_l(V_s - V_l) - g_{\mathrm{Na}} m_\infty^2 h(V_s - V_{\mathrm{Na}}) - g_{\mathrm{KDR}} n(V_s - V_{\mathrm{K}}) + \frac{i_s}{p}. \tag{25}$$

The i_d is a sum of electrotonic coupling $-g_c(V_d - V_s)/(1-p)$, leak current $-g_l(V_d - V_l)$, inward Ca current $-g_{\mathrm{Ca}} s^2 (V_d - V_{\mathrm{Ca}})$, K after-hyperpolarization current $-g_{\mathrm{KAHP}} q(V_d - V_{\mathrm{K}})$, Ca-activated K current $-g_{\mathrm{KCa}} \min([\mathrm{Ca}]/250.0, 1.0)(V_d - V_{\mathrm{K}})$, synaptic current $-i_{\mathrm{syn}}/(1-p)$, and dendrite electrode current $i_{\mathrm{de}}/(1-p)$:

$$r_\infty = 1.0/\{1.0 + 0.28 \exp[-0.062(V_d - 60.0)]\}, \tag{26}$$

$$i_{\mathrm{syn}} = g_{\mathrm{NMDA}} s_{\mathrm{NMDA}} r_\infty (V_d - V_{\mathrm{syn}}), \tag{27}$$

$$i_d = -g_c \frac{(V_d - V_s)}{(1-p)} - g_l(V_d - V_l) - g_{\mathrm{Ca}} s^2 (V_d - V_{\mathrm{Ca}}) - g_{\mathrm{KAHP}} q(V_d - V_{\mathrm{K}}) - g_{\mathrm{KCa}} \min\left(\frac{[\mathrm{Ca}]}{25.0}, 1.0 \right)(V_d - V_{\mathrm{K}}) - \frac{i_{\mathrm{syn}}}{(1-p)} + \frac{i_{\mathrm{de}}}{(1-p)}. \tag{28}$$

Thus the Pinsky-Rinzel neuron is a strongly nonlinear, highly coupled, high-dimensional system. Now we will demonstrate two complementary control algorithms, targeting different spiking behaviors, in this neuron. It appears that the parameter most accessible to external manipulation is the applied soma current i_s, and the variables one can monitor and adjust with greatest ease are the voltages V_s and V_d. So we will demonstrate the efficacy of our methods using *only* these as input in the control algorithms.

The two methods we will introduce complement each other. One is based on the manipulation of a parameter (i_s) and the other involves the manipulation of a state variable (V_s or V_d). Both do not require knowledge of the system's governing equations and are based on the instantaneous value of a single variable of the system (either voltage V_s or V_d).

III. ADAPTIVE FEEDBACK CONTROL

In adaptive control, one applies a feedback loop in order to drive the system parameter (or parameters) to the value(s) required so as to achieve a desired target state [6]. Consider a general N-dimensional nonlinear dynamical system described by the evolution equation

$$\dot{\mathbf{X}} = \mathbf{F}(\mathbf{X}; \mu; t), \tag{29}$$

where $\mathbf{X} \equiv (X_1, X_2, \ldots, X_N)$ are the state variables and μ is the parameter whose value determines the nature of the dynamics. The adaptive control is effected by the additional dynamics

$$\dot{\mu} = \gamma(\mathcal{P}^{\star} - \mathcal{P}), \tag{30}$$

where $\mathcal{P}^{\star}$ is the target value of some variable or property $\mathcal{P}$ (which could be a function of several variables). The value of the proportionality constant γ indicates the ''stiffness of control,'' which determines the strength of the feedback (much like the stiffness of a spring, if one considers the feedback equation to be analogous to the restoring motion of a spring). So the *error signal* $(\mathcal{P}^{\star} - \mathcal{P})$ drives the system to the target state. The scheme is adaptive since in the above procedure the parameters that determine the nature of the dynamics *self-adjust* or adapt themselves to yield the desired dynamics, driven by the ''dynamic feedback.'' Note that the relationship between the parameter μ and the monitored property $\mathcal{P}$ should be monotonic (though it need not be linear, and in fact most often is not) [7].

For the success of the method, the parameter μ in Eq. (30) should be a parameter capable of effecting large dynamical changes such that the feedback can drive its value to a regime that naturally supports the desired dynamics. The property $\mathcal{P}$ should characterize the desired state well, and in addition be simply defined without explicit knowledge of the system's equations of motion. Furthermore, one would like to achieve control without having to monitor a large number of variables. The technique set up by us incorporates all the above features.

Now we will apply this control principle on a Pinsky-Rinzel neuron, targeting different spiking behaviors, i.e., states with different specific interspike intervals $\mathcal{I}$. In this demonstration, we will manipulate the applied soma current i_s, which appears to be the parameter most easily amenable to quick manipulation, i.e., we will attempt to control the neuronal spiking behavior with i_s as our choice for μ in the control Eq. (30). The procedure for reaching and maintaining a particular $\mathcal{I}$, by adjusting the applied current i_s via adaptive feedback, is then as follows: if the desired value of $\mathcal{I}$ is $\mathcal{I}^*$ at all times, then the control equation [with $\mathcal{P} \equiv \mathcal{I}$, $\mathcal{P}^* \equiv \mathcal{I}^*$, and the controlled parmeter $\mu \equiv i_s$ in Eq. (30)] is

$$i_s(n+1) = i_s(n) - \gamma(\mathcal{I}_n - \mathcal{I}^*), \tag{31}$$

where γ is the stiffness of control and $\mathcal{I}_n$ is the current interspike interval, i.e., the time difference between the current spike and its immediately preceding one [8]. This control algorithm has the desired effect of tuning the value of i_s such that the dynamics of the combined equations yields a steady state with $\mathcal{I} = \mathcal{I}^*$.

Note that the control is *stroboscopic*. It is implemented only at the onset of a spike. Whenever a spike occurs, the $\mathcal{I}$ is measured and the feedback mechanism adjusts the current according to Eq. (31).

It should be emphasized that the control algorithm introduced above does not require *a priori* knowledge of the governing equations of the system. The only information necessary to implement adaptive control is the current $\mathcal{I}$ value (i.e., the difference in the time at which the current spike occurs and that at which the previous one had occurred).

Figure 1 shows an example of controlling to a state with low fixed $\mathcal{I}$, namely a state where spiking is frequent and regular. The initial state of the neuron has a current value very far from that which yields the target. Clearly under control dynamics, the neuronal system rapidly reaches the desired state, as is evident from comparing the dynamics with and without control [Figs. 1(a) and 1(b)]. Figure 2 shows the rapid evolution of the parameter to a value that supports the target state, as well as the rapid evolution of property $\mathcal{P} \equiv \mathcal{I}$ to its targeted value.

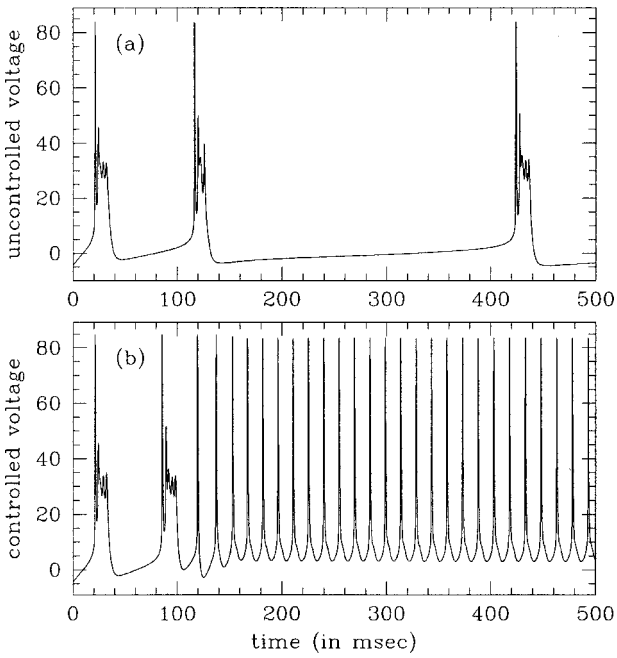

FIG. 1. The time evolution of the membrane potential V_s (in mV) of the Pinsky-Rinzel neuron, for the cases of (a) uncontrolled neuron showing infrequent irregular spiking behavior ($i_s = 1$ nA); (b) the neuron under feedback control, with target $\mathcal{I}^* = 15$ ms and stiffness of control $\gamma = 0.05$ in Eq. (31). Note that the control rapidly leads to spiking at regular intervals of 15 ms, as desired.

Once the system achieves the target, it remains there and the control equation is ''switched off'' [as the error signal is naturally zero in Eq. (31)]. If the parameters begin to drift (for instance, due to environmental fluctuations), the control automatically becomes effective again (as the error signal becomes nonzero again) and it readily brings the system back to the desired state.

The stiffness γ determines how rapidly the system is controlled. The control time, defined as the time required to reach the desired state, is crucially dependent on the value of γ. Numerical experiments show that for small γ, the recovery time is inversely proportional to the stiffness of control (see Fig. 3).

If we wish to target a more irregular firing state, we have to set a target $\mathcal{I}$ of larger than 30 ms, as the system can only support irregular firing beyond that $\mathcal{I}$, and so the adaptive mechanism leads to fluctuating current i_s, which in turn leads to irregular firing around a mean $\mathcal{I}^*$. Thus we can achieve the desired effect of obtaining a state with very irregular spikes (see Fig. 4 for a representative example of this ''anticontrol'').

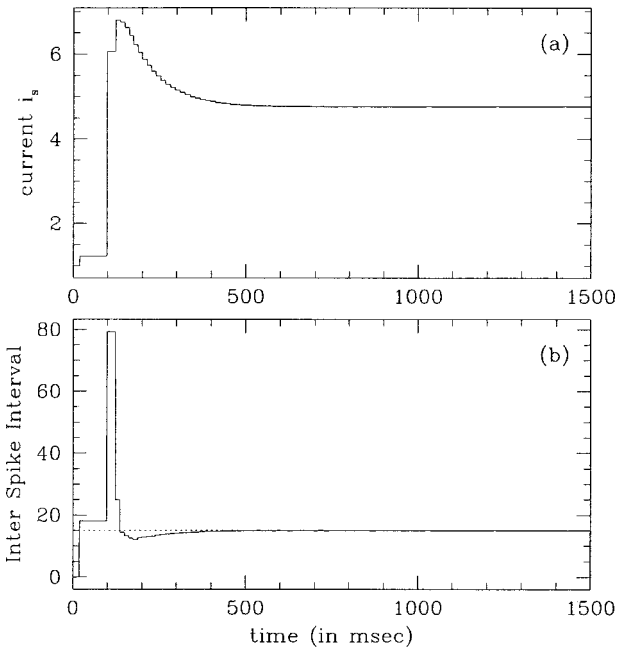

FIG. 2. The time evolution of (a) the soma current i_s (in nanoamperes) and (b) the interspike interval $\mathcal{I}$ (in ms) for the Pinsky-Rinzel neuron under adaptive feedback control with $\mathcal{I}^*=15$ ms and $\gamma=0.075$ in Eq. (31). The dashed line in (b) shows the target ISI of 15 ms. The initial soma current is $i_s=1.0$ nA, which when uncontrolled yields large and very irregular $\mathcal{I}$. Note that the control switches off [as the error tem in Eq. (31) goes to zero] when the system reaches the target state (at $t\sim 400$ ms).

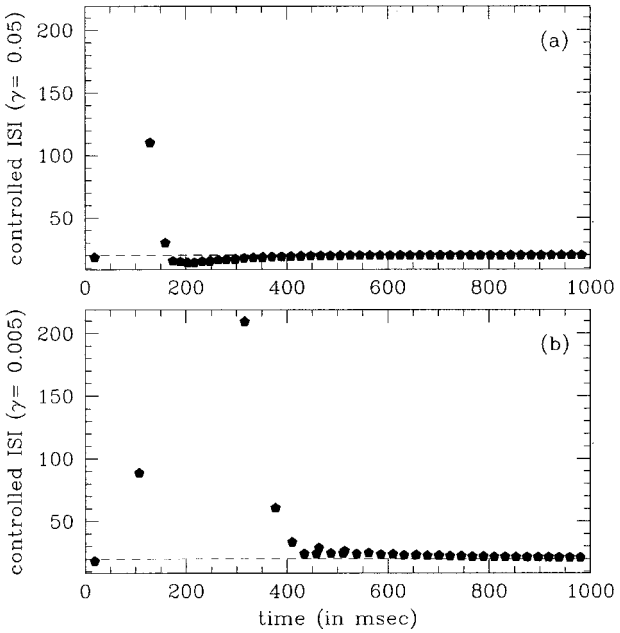

FIG. 3. The time evolution of the interspike interval $\mathcal{I}$ (in ms) for the Pinsky-Rinzel neuron under adaptive feedback control with $\mathcal{I}^*=20$ ms, and stiffness of control γ equal to (a) 0.05 and (b) 0.005 in Eq. (31). The dashed line shows the target $\mathcal{I}$ of 20 ms. Note that with $\gamma=0.05$, the target state is achieved in about half the time as compared with $\gamma=0.005$.

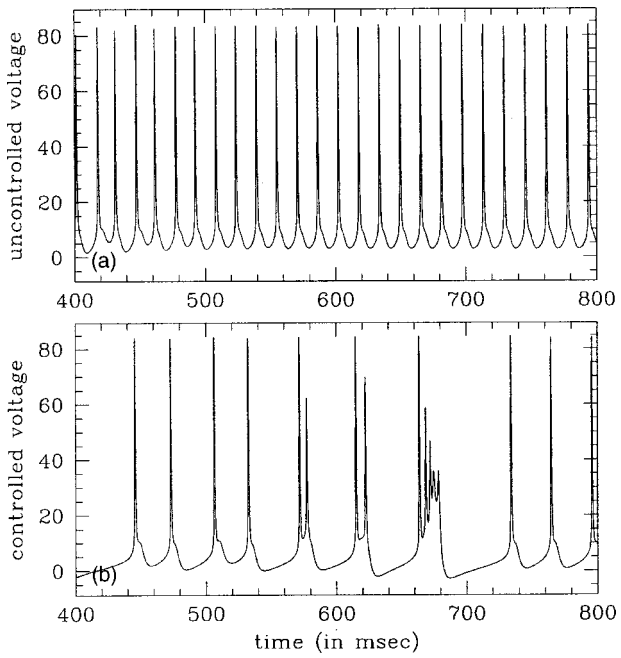

FIG. 4. The time evolution of the neuronal membrane potential V_s (in mV) for the cases of (a) the uncontrolled neuron showing very frequent and regular spiking ($i_s=4.0$ nA); (b) the neuron under feedback ''anticontrol,'' where the target is a state with irregular firing. Here the target is set at $\mathcal{I}^*=40$ ms and stiffness of control $\gamma=0.01$ in Eq. (31). Note that the control rapidly leads to irregular and infrequent spiking, as desired.

In real experiments, it is conceivable that the ISI may not be measured very accurately. Thus the technique outlined above should be reliable with respect to noise in ISI determination, in order to be useful. We have checked that the method indeed is successful even if the ISI fed into the feedback loop has a noisy spread amounting to up to 5% of the targeted $\mathcal{I}$.

Finally, note that this control method has one limitation: if the system does not have any parameter regime yielding the targeted dynamical behavior, the adaptive control will fail to achieve that particular target. So the method is capable of achieving only those targets that have a stable basin of attraction somewhere in parameter space. This is usually not much of a limitation, though, as nonlinear systems generically support many different dynamical behaviors in different parameter regimes, as is evident from the rich bifurcation structure in parameter space of most nonlinear systems. So in this sense, adaptive control works like an efficient search algorithm for varied dynamical characteristics in parameter space, as is the case in this neuronal model for both regular and irregular firing targets [8].

IV. THRESHOLD CONTROL OF A STATE VARIABLE

Now we describe how threshold mechanisms can be effectively employed to control neuronal systems onto stable fixed spiking patterns by manipulating not a parameter but a state variable of the system.

First we discuss the general strategy of using threshold mechanisms as a means of control [9]. Consider a general N-dimensional dynamical system, described by the evolution equation $\dot{\mathbf{x}}=F(\mathbf{x};t)$, where $\mathbf{x}\equiv(x_1,x_2,\ldots,x_N)$ are the state variables, and variable x_i is chosen to be monitored and manipulated. The prescription for threshold control in this system is as follows: control will be triggered whenever the value of the monitored variable exceeds the critical threshold x^* (i.e., when $x_i>x^*$) and the variable x_i will then be reset to x^*. No knowledge of $F(\mathbf{x})$ is involved, and no computation is needed to obtain the necessary control. The dynamics continues until the next occurrence of x_i exceeding the threshold, when control resets its value to x^* again.

Note that the threshold control is stroboscopic as the threshold condition is checked at finite intervals of τ_c. Furthermore resetting the value of the variable to x^* should be very fast compared to the natural dynamics of the uncontrolled system. So the state variables most accessible to external manipulation are the most suitable candidates for thresholding.

In the context of neuronal systems, it is unrealistic to implement the threshold mechanism on the gating variables or the Ca levels as it is unlikely that one can manipulate these externally with ease. On the other hand, it is natural to try and implement the threshold action on the somatic or dendritic voltages V_s or V_d, as they are much more accessible to measurement and monitoring. Thus we demand that variable V_s or V_d must not exceed a prescribed threshold value $V^*(1<V^*<20\,\mathrm{mV})$ and we examine the scope of this mechanism to yield regular firing behavior.

Figures 5–9 show some representative results of this threshold action for a range of threshold values. It is clear that the mechanism manages to yield complete regularity, as compared with the very irregular and infrequent firing behavior of the neuron with no thresholding, with the thresholded variable having the ability to drag the rest of this high-dimensional system to regular dynamical behavior (see Fig. 5). The characteristics of the thresholded states, for instance its ISI, are determined completely by the threshold V^* and the interval of control τ_c. The threshold mechanism typically yields two types of behavior: periodic states (with period τ_c) and states with regular spiking (with interspike intervals ranging from about 14 to 60 ms). Low threshold and frequent checking of the threshold condition (i.e., small τ_c) lead to the first dynamics and higher thresholds and larger τ_c lead to regular firing states.

Figure 6 displays the behavior of the neuron under threshold mechanism on the dendritic potential V_d. It is clear that the threshold mechanism very effectively brings the system to a regular state, as compared with the very irregular and infrequent firing behavior of the neuron with no thresholding, given in Fig. 5(a). As mentioned before, the characteristics of the thresholded states are determined completely by the threshold V^* and the interval of control τ_c (i.e., the interval at which the threshold condition is checked). For thresholds up to $V^*\sim5$ mV, one obtains periodic states with periodicity equal to τ_c, when control intervals are short ($\tau_c\sim0.1$ ms), as is evident in the example in the inset of Fig. 6(b). When the threshold condition is checked and reset infrequently (say $\tau_c\sim1$ ms), one obtains spikes at exactly regular intervals [see Fig. 6(a)].

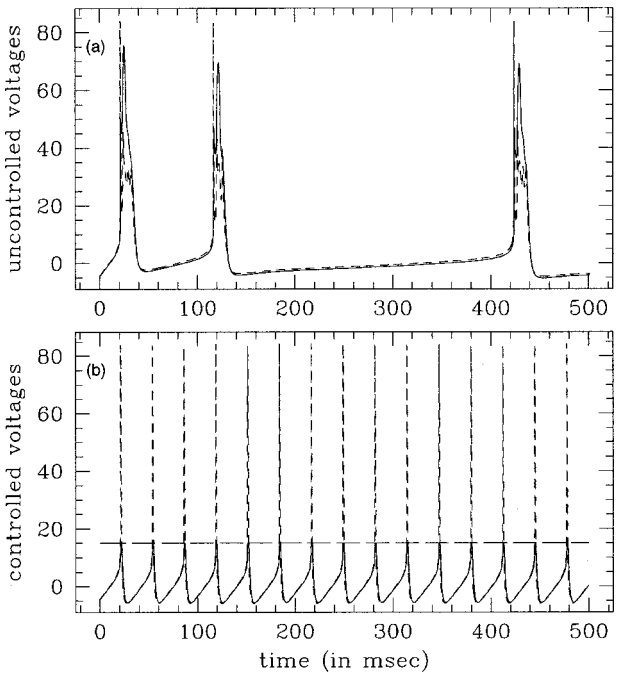

FIG. 5. The time evolution of the voltages V_s and V_d (in mV) for the Pinsky-Rinzel neuron for the cases of (a) the uncontrolled neuron showing infrequent and irregular spiking behavior; (b) the same neuron, with voltage V_d under threshold control, with threshold $V^*=15$ mV (here $i_s=1$ nA). Clearly, the controlled neuron spikes at very regular intervals. The solid lines show V_d(—) and the dashed lines show V_s (---). The interval at which the threshold condition is checked is 0.1 ms. The threshold voltage of $V^*=15$ mV is shown by a dashed line (––).

Beyond a threshold value of about 5 mV, all thresholds yield regular spiking states, even when control is implemented frequently (see Figs. 7 and 8). Note that these regular firing states have interspike interval values ranging from about 14 to ~60 depending on the applied soma current i_s (see Fig. 7). Interestingly, the relationship between current i_s and the interspike interval is a *very well defined power law*,

$$\mathcal{I}\sim i_s^{\nu}, \tag{32}$$

where the exponent $\nu\sim0.6$ (see Fig. 8).

For thresholding on the somatic voltage V_s, one obtains periodic states for short control intervals ($\tau_c\sim0.1$ ms) for thresholds up to about $V^*\sim20$ mV [see Fig. 9(b)]. When control is implemented infrequently, i.e., $\tau_c\sim1$ ms, one obtains (a) periodic states as usual for small thresholds $V^*<10$ mV, and (b) regular spiking states for large thresholds ($V^*\sim10$ mV), as is clearly seen in Fig. 9(a).

When the threshold is very large (close to the upper limits of the spike, $V^*>20$ mV) or the interval of implementing control is very large ($\tau_c>1$ ms), the system under threshold mechanism yields slightly irregular spiking states, with mildly fluctuating ISI (though still much more regular than the unthresholded system).

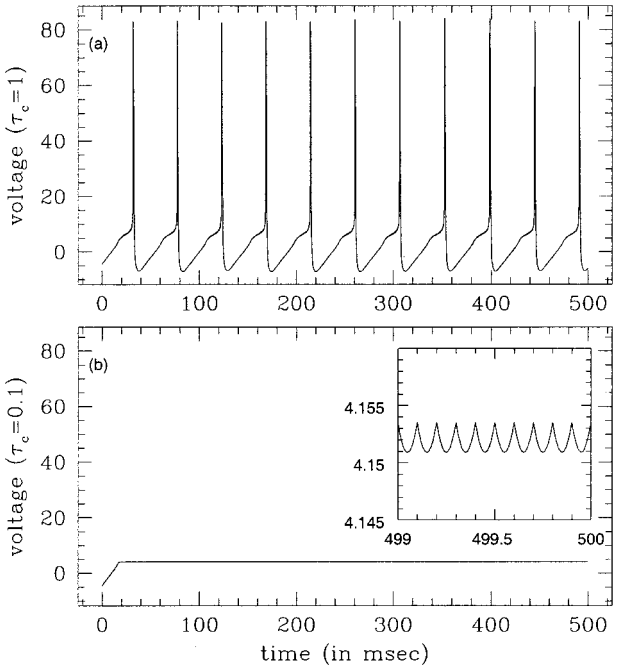

FIG. 6. The time evolution of the voltage V_s (in mV) for a Pinsky-Rinzel neuron, with V_d under threshold mechanism. Here threshold $V^*=3$ mV and the interval of control τ_c is equal to (a) 1 ms and (b) 0.1 ms. The inset in (b) shows a blown up section of the figure, clearly showing a periodicity of τ_c.

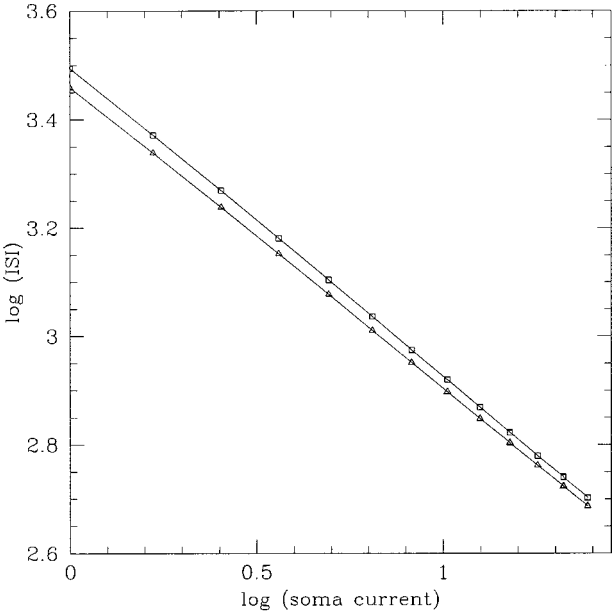

FIG. 8. Interspike interval ISI (in ms) vs soma current i_s (in nanoamperes) for the Pinsky-Rinzel neuron under threshold control of voltage V_d. (The base of the logarithm in the plot is *e*.) The interval at which the threshold condition is checked is 0.1 ms. The triangles represent a threshold value of $V^*=10$ mV and the squares represent $V^*=20$ mV.

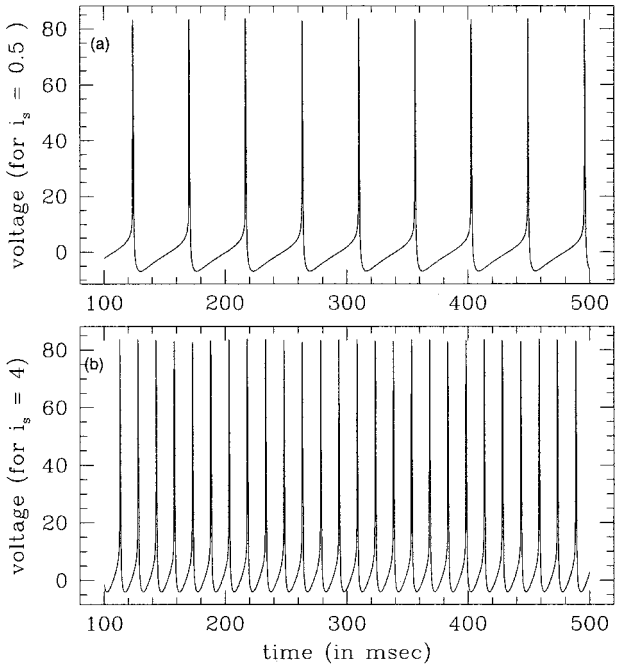

FIG. 7. The time evolution of the voltage V_s (in mV) for a Pinsky-Rinzel neuron with voltage V_d under threshold control, with threshold $V^*=10$ mV, $\tau_c=0.1$, and the applied soma current equal to (a) $i_s=0.5$ nA and (b) $i_s=4$ nA. Clearly the periodicity of spiking is very different for the two cases.

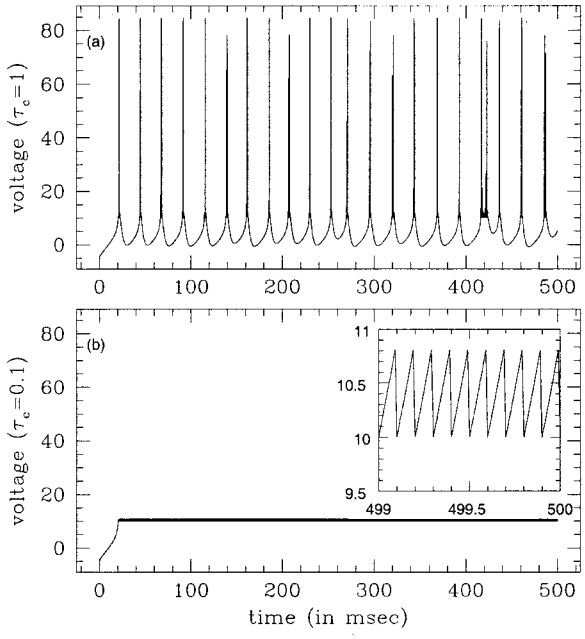

FIG. 9. The time evolution of the voltage V_s (in mV) for a Pinsky-Rinzel neuron, with V_s under threshold mechanism. Here threshold $V^*=10$ mV and the interval for stroboscopic checking of the threshold condition equal to (a) 1 ms and (b) 0.1 ms. The inset in (b) shows a blown up section of the figure, clearly showing a periodicity of τ_c.

Note that the control transience is very short in threshold control. In threshold control, the system does not have to be close to any particular unstable fixed point before implementing the control. Once a specified state variable exceeds the threshold, it is caught immediately in a stable orbit (see Fig. 5). So there is no significant interval between the onset of control and the achievement of control, as a wide interval is open to targeting. Also, unlike most other control methods, *threshold control does not entail any run-time computation during control*.

The perturbations involved in threshold control are not large compared to the voltage spikes, which are of the order of 80 mV [see Fig. 5(a)]. We give a few representative control perturbations here: for instance, when the threshold is 40 mV and $\tau_c = 0.01$, the *maximum* perturbation required to effect control is ~ 0.5 mV, i.e., only ~ 0.005 times the uncontrolled spike height. The resetting occurs stroboscopically in intervals of 0.01 ms, over a period of 0.5 ms, every 26 ms (which is the period of spiking obtained from this threshold value). That is, for about 25.5 ms in an interval of 26 ms, the threshold control does not need to act.

We find that the maximum perturbation required for thresholding is inversely proportional to τ_c. So in order to reduce the maximum perturbation, we can make the stroboscopic control more frequent. For instance, in the example above, if we wanted the maximum perturbation to be only 0.05 mV (i.e., ~ 0.0005 times the spike height), we must make $\tau_c = 0.001$.

For lower threshold values which yield spiking at periodicity equal to τ_c, the maximum perturbation is again inversely proportional to τ_c. So again the maximum perturbation can be made small by making the stroboscopic control more frequent. For instance, for threshold at 0.1 mV, with $\tau_c = 0.01$ ms, the maximum perturbation is 0.0074 mV (i.e., 10^4 times smaller than the uncontrolled spike height), while for $\tau_c = 0.0001$ ms the maximum perturbation is as low as 0.000 074 mV.

We also checked that the method works for slightly delayed threshold action, which is a scenario where the variable is brought down to the threshold value after a small delay (as is conceivable in real setups where there may be a small delay between the detection of the crossing of the threshold condition and the resetting of the state variable). We find that the method is still as effective.

The basis of the marked success of the threshold method is clear for one-dimensional maps: $x_{n+1} = f(x_n)$. It is best rationalized through the fixed points of the effective map obtained from the chaotic map under threshold mechanism, i.e., with the additional constraint of $f(x_n) = x^*$ if $f(x_n) > x^*$. The fixed points of this ''beheaded'' map under varying heights of truncation (i.e., different thresholds) give different superstable periods [9]. In terms of probability densities, the chaotic map under the threshold mechanism will map large intervals onto severely contracting regions, and this makes the transient period for control very small and the controlled periodic states superstable.

One of the significant unanswered questions regarding threshold control is the following: it is not clear why the method works so well for higher-dimensional systems, where only one state variable is amenable to threshold control. Unlike in one-dimensional (1D) maps where the orbit is trapped in a cycle as soon as x_n exceeds threshold, in higher dimensions we are not guaranteed that the remaining variables will take the same value at the next threshold control event. So the multidimensional orbit typically will not get trapped in a cycle as soon as one of its variables exceeds the threshold. The issue in higher-dimensional systems then is whether or not the thresholded state variable (which is essentially like a pinned variable) can drag the rest of the system variables to some fixed dynamical behavior.

Last, note that this control method, though very rapid and powerful, is ultimately limited by the systems's dynamical characteristics. If the system's dynamics does not yield a certain desired regular behavior under any threshold, this control method will fail to achieve that particular target. Most often, though, the richness of chaos allows the dynamics to be ''pruned'' to many different kinds of dynamical behavior under the threshold mechanism. While for 1D maps it can be proved that all possible periods can in principle be obtained under varying thresholds [9], this cannot be shown for continuous-time multidimensional systems. One then has to investigate the scope of the threshold method on different state variables in different physical situations, case by case. This was the motivation behind our study on a realistic neuronal model here, and the investigation has provided clear evidence of the capacity of thresholding on the membrane potentials to yield regular spiking of different periods.

V. DISCUSSION

In summary, here we have presented control algorithms that can be used to achieve desired firing behavior in a neuronal system. The methods complement each other: one involves the manipulation of only a parameter, the applied soma current, and the other involves the manipulation of only a state variable, the membrane potential. Both techniques have the advantage that they are not measurement-intensive nor do they involve much run-time computation, as knowledge of only the interspike interval is necessary to implement control. The power and robustness of the techniques is demonstrated for targets ranging from quiet ''nonspiking'' states to regular firing at different interspike intervals, as well as for ''anticontrol'' to irregular firing patterns.

The control of neuronal systems, while in its infancy, is of vital importance for both the understanding and the manipulation of neural dynamics. Potential applications range from the suppression of seizures to computing with living neural tissue. While in naturally occurring systems isolated neurons rarely appear, there are technological developments in the interfacing of single/few neurons to silicon, as well as experiments on single neurons, which make the control of single neurons of considerable interest. The extensive effort to utilize single or groups of isolated neurons (interfaced to silicon substrates) for various purposes (including computation) is a significant motivation for elucidating mechanisms through which control can be implemented in such single

neuronal systems. Additionally, this is the first step in the development of higher-dimensional, spatial methods of control for real neuronal arrays and assemblies. Thus the important fact is that the model chosen for control here closely models the types of neurons that are being interfaced to artificial substrates (such as silicon), and therefore this study has relevance in the design and implementation of artificial, neuroengineered living neural systems.

[1] T. Shinbrot *et al.*, Nature (London) **363**, 411 (1993); A. Garfinkel *et al.*, Science **257**, 1230 (1992); S. J. Schiff *et al.*, Nature (London) **370**, 615 (1994); K. Hall *et al.*, Phys. Rev. Lett. **78**, 4518 (1997).

[2] *Patterns, Information and Chaos in Neuronal Systems*, edited by B. J. West (World Scientific, Singapore, 1993), and references therein.

[3] P. Pinsky and J. Rinzel, J. Comput. Neurosci. **1**, 39 (1994).

[4] R. Traub and R. Miles, *Neuronal Networks of the Hippocampus* (Cambridge University Press, New York, 1991).

[5] J. F. Lindner and W. L. Ditto, in *Proceedings of the Third Technical Conference on Nonlinear Dynamics (Chaos) and Full-Spectrum Processing, Mystic, CN*, edited by R. A. Katz, AIP Conf. Proc. No. 375 (AIP, New York, 1996), p. 709.

[6] B. Huberman and H. L. Lumer, IEEE Trans. Circuits Syst. **37**, 547 (1990); S. Sinha *et al.*, Physica D **43**, 118 (1990); Phys. Lett. A **156**, 475 (1991); R. Ramaswamy *et al.*, Phys. Rev. E **57**, R2507 (1998); S. Sinha and N. Gupte *ibid.* **58**, R5221 (1998).

[7] If the dependence of $\mathcal{P}$ on parameter μ is not by and large monotonic, one has to explicitly incorporate a fluctuating sign in the control equation (namely the stiffness γ is positive or negative depending on the local change of $\mathcal{P}$ with respect to μ). This would make the control algorithm more complicated, and necessitate additional measurements and run-time computation.

[8] The spikes are obtained from the onset of the rise in a voltage via a threshold crossing criterion. Here, when the neuronal voltage (V_d or V_s) crosses 5 mV on the rise, it is taken to be the onset of a spike. Importantly, the method is not sensitive to different means of determining the spikes, e.g., to different thresholds for the threshold-crossing criterion. The method is indeed robust to imprecision in the spike determination.

[9] S. Sinha and D. Biswas, Phys. Rev. Lett. **71**, 2010 (1993); L. Glass and W. Zeng, Int. J. Bifurcation Chaos Appl. Sci. Eng. **4**, 1061 (1994); S. Sinha, Phys. Rev. E **49**, 4832 (1994); Phys. Lett. A **199**, 365 (1995).